ACS APPLIED MATERIALS & INTERFACES

Research Article

www.acsami.org

Poly(2-Vinyl-4,4-dimethylazlactone)-Functionalized Magnetic Nanoparticles as Carriers for Enzyme Immobilization and Its Application

Xiaoyu Mu,[†,‡] Juan Qiao,[†] Li Qi,[*,†] Ping Dong,[§] and Huimin Ma[†]

[†]Beijing National Laboratory for Molecular Sciences, Key Laboratory of Analytical Chemistry for Living Biosystems, Institute of Chemistry, Chinese Academy of Sciences, Beijing 100190, P.R. China

[‡]Graduate School, University of Chinese Academy of Sciences, Beijing 100049, P. R. China

[§]Research Centre of Plastic Surgery Hospital, Chinese Academy of Medical Sciences & Peking Union Medical College, Beijing 100144, P. R. China

Supporting Information

ABSTRACT: Fabrication of various efficient enzyme reactors has triggered increasing interests for its extensive applications in biological and clinical research. In this study, magnetic nanoparticles were functionalized by a biocompatible reactive polymer, poly(2-vinyl-4,4-dimethylazlactone), which was synthesized by reversible addition−fragmentation chain transfer polymerization. Then, the prepared polymer-modified magnetic nanoparticles were employed as favorable carriers for enzyme immobilization. L-Asparaginase was selected as the model enzyme to fabricate the enzyme reactor, and the prepared enzyme reactor exhibited high loading capacity of 318.0 μg mg^{-1} magnetic nanoparticle. Interestingly, it has been observed that the enzymolysis efficiency increased slightly with the lengthened polymer chain, resulting from the increased immobilization amount of enzyme. Meanwhile, the immobilized enzyme could retain more than 95.7% activity after 10 repeated uses and maintain more than 72.6% activity after 10 weeks storage. Moreover, an extracorporeal shunt system was simulated to estimate the potential application capability of the prepared L-asparaginase reactor in acute lymphoblastic leukemia treatment.

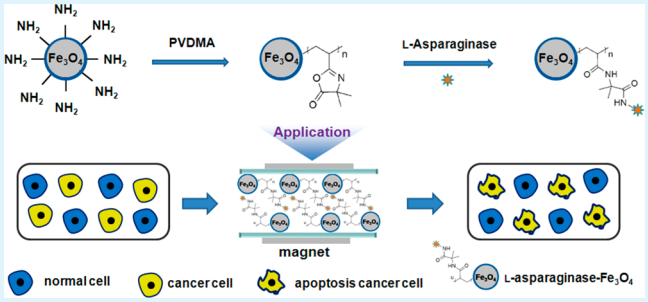

KEYWORDS: *poly(2-vinyl-4,4-dimethylazlactone), magnetic nanoparticles, enzyme immobilization, L-asparaginase*

1. INTRODUCTION

Enzymes are ubiquitous natural biocatalysts, and they are accepted to be more economical and environmentally friendly because of high efficiency, low cost, excellent selectivity, and shorter synthetic routes compared with the chemical catalysts.[1] Notwithstanding all these advantages, the application of enzymes in various industrial processes is often hampered by the unsatisfactory operational and storage stability, the extensive incubation time and the difficulties in recovery or reuse.[2] Generally, these drawbacks can be conquered by immobilization of enzymes on the prefabricated supports. In the past decades, various materials have been developed as efficient supports for enzyme immobilization, such as porous monolith, organic membrane, silicon matrix, and nanomaterials.[3] Among these supports, nanomaterials generally provide a large surface area for immobilization of enzyme and have been prospected as the promising carriers for enzyme stabilization.[4] Especially, the magnetic nanoparticles modified by polymer brushes, which possess numerous active sites on the polymer shells, are considered to be a fascinating alternative for enzyme immobilization due to their outstanding advantages, including high loading capacity, convenient isolation from reaction mixture, favorable biocompatibility and good reusability.[5] Up to now, a variety of polymer brushes, such as poly(acrylic acid), chitosan, poly(ethylene glycol) and poly(glycidyl methacrylate), have been successfully employed to functionalize the surface of magnetic nanoparticles for immobilization and fabrication of highly active enzyme reactors.[5−7] However, enzyme conjugation on these polymer-modified magnetic nanoparticles still bears some inadequacies: I) the reaction conditions are often rigorous and a long reaction time is generally needed; II) there are restricted active sites for enzyme immobilization, resulting in low immobilization efficiency; III) the species of reactive polymer are limited. Therefore, exploration and fabrication of novel reactive polymer-modified magnetic nanoparticles for rapid and efficient enzyme immobilization is of great significance.

2-Vinyl-4,4-dimethyl azlactone (VDMA)-based polymers serve as convenient reactive scaffolds with the dimethylazlactone rings being readily opened by nucleophiles, including

Received: September 14, 2014
Accepted: October 31, 2014
Published: October 31, 2014

amines, hydroxyls and thiols.[8,9] The azlactone functionality of VDMA can readily react with the amino or thiol groups of proteins thereby enabling their rapid and efficient immobilization. Therefore, poly(2-vinyl-4,4-dimethyl azlactone) (PVDMA) brushes are found to be potential templates, which can provide the surface of materials with reactive functionalities required for enzyme immobilization. Compared with the activated ester chemistry, one main advantage about the azlactone functionality is that the ring-opening reaction with nucleophiles is an addition reaction, and this provides a better atom economy and avoids the need for separation of a leaving group.[8] As one kind of flexible reactive templates, the VDMA has been used as a monomer to provide the pore surface of the monolith with reactive functionalities required for enzyme immobilization.[10,11] However, the cross-linking of the monomer in the monolith might embed the reactive functionality of VDMA and limit the immobilization efficiency. Recently, it has been reported that the polymer brushes modified on the surface of magnetic nanoparticles could provide numerous binding sites and further function as scaffolds to support three-dimensional enzyme immobilization.[5] As a result, both the loading amount and accessibility of the immobilized enzyme is remarkably increased. Therefore, PVDMA brushes are considered to be a promising and versatile reactive polymer for modification of the surface of magnetic nanoparticles, further being applied in fabricating efficient enzyme reactors.

L-Asparaginase, which specifically catalyzes the hydrolysis of L-asparagine producing L-aspartic acid and ammonia, has been extensively employed as a chemotherapy agent for treatment of acute lymphoblastic leukemia.[12] Notwithstanding its high therapeutic efficacy, some defects are still existed in the use of L-asparaginase, including hypersensitivity reactions and a short half-life, resulting in need for frequent dosing.[13] To overcome these drawbacks, the native L-asparaginase has been immobilized on various carrier materials. Accordingly, extracorporeal shunt systems have been developed using enzyme immobilized on nylon tubing, collagen matrix, polycarboxylic gel and so on.[14−16] Considering the outstanding advantages of reactive polymer-grafted magnetic nanoparticles, including convenient manipulation, high functionality, enhanced activity, excellent stability, and good reusability, they could possess powerful capability in efficiently immobilizing L-asparaginase.

In this work, since PVDMA is well-known for its good biocompatibility and widespread biomedical applications, it was employed to modify the surface of the magnetic nanoparticles with multiple reactive groups. Then, L-asparaginase as the model enzyme was conjugated onto the PVDMA-grafted magnetic nanoparticles to fabricate an enzyme reactor. Additionally, the performance of the proposed enzyme reactor (including enzyme activity, reusability, and stability) was evaluated using a chiral ligand exchange capillary electrophoresis (CLE-CE) protocol with novel amino acid ionic liquids (AAILs) as chiral ligands. Furthermore, the extracorporeal shunt system was simulated by incubating the human serum samples with the prepared enzyme reactor.

2. EXPERIMENTAL SECTION

2.1. Chemicals. All the amino acid (AA) enantiomers, dansyl chloride (Dns-Cl), coomassie brilliant blue G-250, and phosphotungstic acid (PTA) were purchased from Sigma-Aldrich Chemical Co. (St. Louis, USA). L-Asparaginase (from *Escherichia coli*) which consisted of 303 AAs and possessed a molecular mass of 31 731 Da was obtained from ProSpec-Tany Techno-Gene (Rehovot, Israel). *N*-Ethyl-*N*-methylpyrrolidinium bromide ([PP1,2][Br]), *N*-butyl-*N*-methylpyrrolidinium bromide ([PP1,4][Br]), *N*-hexyl-*N*-methylpyrrolidinium bromide ([PP1,6][Br]), and *N*-octyl-*N*-methylpyrrolidinium bromide ([PP1,8][Br]) were supplied by Lanzhou Institute of Chemical Physics (Lanzhou Greenchem ILS, LICP, CAS, P.R. China). The monomer VDMA was bought from Beijing Institute of Coollight Fine Chemicals (Beijing, China). 2,2′-Azobis(isobutyronitrile) (AIBN) was purchased from Shanghai Chemical Plant (Shanghai, China) and refined before use. Ferric chloride hexahydrate ($FeCl_3{\cdot}6H_2O$) was obtained from Xilong Chemical Company (Guangdong, China). Ferrous chloride tetrahydrate ($FeCl_2{\cdot}4H_2O$) was from Tianjin Damao Chemical Reagent Factory (Tianjin, China). Zinc sulfate, boric acid, lithium carbonate, tris (hydroxymethyl) aminomethane (Tris), tetraethyl orthosilicate (TEOS), 3-aminopropyltriethoxysilane (APTES), sodium hydroxide, hydrochloric acid, anhydrous ethanol, methanol, tetrahydrofuran (THF), 2-propanol, hexane, carbon disulfide, chloroform, acetone, acetonitrile, dichloromethane (DCM), 1-dodecanethiol, tricaprylylmethylammonium chloride, *n*-hexane and other reagents were all purchased from Beijing Chemical Factory (Beijing, P.R. China). Deuterium oxide (D_2O, 99%) and acetonitrile-d_3 were from Cambridge Isotope Laboratories (Massachusetts, USA). All the chemical reagents used in this work were of analytical grade.

2.2. Instrumentation. The Fourier transform infrared (FT-IR) spectra were recorded on a Bruker Tensor-27 spectrophotometer in the wavenumber range from 4000 to 400 cm^{-1} under ambient conditions. The size and morphology of the particles were observed by transmission electron microscope (TEM, JEOL JEM-2010) at an acceleration voltage of 200 kV. Samples were dropped on a carbon-coated 200 mesh copper grid, followed by drying at ambient conditions before it was placed to the sample holder on the microscope. Moreover, to visualize the polymer coating, negative staining of the TEM sample was conducted with PTA as staining agent, and the sample was observed by a JEM-100CXII electron microscope at an acceleration voltage of 100 kV. Magnetic measurement was conducted on a Lakeshore 7307 vibrating sample magnetometer (VSM) at room temperature. MALDI-TOF MS analysis was conducted on a Bruker Ultraflextreme MALDI-TOF/TOF mass spectrometer (Bruker Daltonics, Germany) equipped with a 355 nm and solid-state Nd:YAG/355 nm SmartBeam laser. Gel permeation chromatography (GPC) experiments were performed on a Waters 1515 HPLC solvent pump equipped with a Waters 2414 differential refractometer detector and a set of Waters Styragel columns. THF was employed as the eluent at a flow rate of 1.0 mL/min with polystyrene calibration. All the separation experiments were performed on a capillary electrophoresis (CE) system composed of a UV detector (Rilips photoelectricity factory, Beijing, China), a 1229 HPCE high voltage power supply (Beijing institute of new technology and application, Beijing, China) and a HW-2000 chromatography workstation (Qianpu software, Nanjing, China). The fused-silica capillaries were purchased from Yongnian optical fiber factory (Hebei, China) with a total length of 60 cm (effective length 45 cm, 75 μm i.d. × 365 μm o.d.). The PVDMA content on the surface of the magnetic nanoparticles was determined by a thermogravimetric analyzer (TGA 7, PerkinElmer, USA) with a temperature range from 50 to 750 °C at a heating rate of 20 °C/min in air. The dynamic light scattering (DLS) measurements were performed using a Zetasizer Nano ZS (Malvern Instruments).

2.3. CE Analysis. The new capillary was treated with 1.0 M HCl, 1.0 M NaOH and water in sequence. Between runs, the capillary was washed with 1.0 M HCl, water, 1.0 M NaOH, water, and running electrolyte for 2 min, respectively. The enantiomeric AA samples were prepared in 40.0 mM lithium carbonate buffer (adjusted to pH 9.5 with 0.1 M HCl) at a concentration of 2.0 mg/mL unless otherwise noted, then diluted to the desired concentrations in the range of 10−10^4 folds with the lithium carbonate buffer for further analysis. It should be mentioned that L-enantiomers were fortified to racemic AAs to validate the migration orders of AA enantiomers. Samples were siphoned to the capillary from the cathode for 8 s at 15 cm height. Then they were separated at a voltage of −20 kV and detected at

Table 1. Characterization Results of PVDMA Homopolymers

sample	polymerization time (h)	conversion (%)[a]	polymerization degree[b]	determined M_w[c]	$M_{n,GPC}$[d]	$M_{w,GPC}$[d]	PDI[d]
PVDMA-1	12	64	68	10652	2773	2795	1.21
PVDMA-2	24	78	79	14803	3927	3962	1.06
PVDMA-3	36	95	102	18792	4715	4731	1.17

[a]The conversion was determined by ^{1}H NMR of reaction sample with acetonitrile-d_3 as solvent by comparing the monomer signal at 6.34 ppm (^{1}H) with the methyl group signal of the dimethylazlactone ring at 1.42 ppm (6 H). [b]Polymerization degree was calculated by^{1}H NMR of the obtained polymer with acetonitrile-d_3 as solvent by comparing the signal of the methyl group of the CTAs at 0.88 ppm (3H) with the signal of the methyl group of the dimethylazlactone ring at 1.45 ppm (6H). [c]The molecular weight (M_w) was obtained by MALDI-TOF MS analysis. [d]The $M_{n,GPC}$, $M_{w,GPC}$, and polydispersity index (PDI) were determined by GPC

anode side. Unless otherwise specified, the running buffer in CE for this study was composed of 100.0 mM boric acid, 5.0 mM ammonium acetate, 3.0 mM zinc sulfate and 15.0 mM AAIL, adjusted to pH 8.4 with Tris.

Derivatization of AAs with Dns-Cl was performed according to our previous literature.[17] Briefly, 20 μL of 1.5 mg/mL Dns-Cl was mixed with 20 μL of AAs and 20 μL 40.0 mM lithium carbonate buffers (pH 9.5, adjusted with 1.0 M HCl) in a 200 μL vial. The mixture was reacted under microwave radiation (480 W) for 4 min. Then the derivatization reaction was terminated after adding 5 μL of 2% ethylamine. All the samples were kept at 4 °C before injection.

2.4. Fabrication of L-Asparaginase Reactor. *2.4.1. Synthesis of PVDMA.* The RAFT agent *S*-1-dodecyl-*S*′-(α,α′-dimethyl-α″-acetic acid)trithiocarbonate (CTAm) was synthesized according to the literature.[18] The VDMA homopolymers were prepared by reversible addition−fragmentation chain transfer (RAFT) polymerization according to the following procedures as described in the literature with minor modification (Supporting Information Scheme S1).[19,20] Briefly, VDMA (1.04 g, 7.5 mmol), CTAm (25.50 mg, 0.07 mmol) and AIBN (1.20 mg, 0.007 mmol) were dissolved in 3 mL of acetonitrile, and stirred in a preheated oil bath at 70 °C under the protection of nitrogen for the desired time (12, 24, and 36 h). Then the resultant was precipitated in hexane and the product was dried in vacuo.

2.4.2. Preparation of Magnetic Nanoparticles. The magnetic nanoparticles were synthesized according to the procedure as reported by Massart and Cabuil.[21] $FeCl_3{\cdot}6H_2O$ (5.40 g, 20.0 mmol) and $FeCl_2{\cdot}4H_2O$ (1.98 g, 10.0 mmol) were dissolved in 100 mL of deionized water. Then the pH of the solution was adjusted to 12 by the addition of 25% ammonia, and the solution was stirred to react for at 65 °C 3 h. The resultant Fe_3O_4 nanoparticles were washed with water for several times until the pH was neutral. Then these obtained nanoparticles were washed with ethanol and dried in vacuo.

2.4.3. Preparation of SiO_2−Fe_3O_4 Nanoparticles. To improve the stability and biocompatibility of magnetic nanoparticles, the surface of nanoparticles was coated with a silica layer as the process described in the literature.[22] Briefly, 0.5 g of Fe_3O_4 nanoparticles were added into a mixture of 100 mL ethanol and 25 mL water, then 2.5 mL 25% ammonia solution and 5 mL TEOS were added dropwise in sequence. The product was washed for several times by water and ethanol in turn after reaction for 24 h, and dried under vacuum.

2.4.4. Preparation of APTES−Fe_3O_4 Nanoparticles. SiO_2−Fe_3O_4 nanoparticles (0.5 g) were added into 50 mL of ethanol, and then 6 mL of APTES was added dropwise. The mixture was reacted at room temperature (25 °C) for 24 h. The obtained nanoparticles were washed with ethanol for several times and dried under vacuum.

2.4.5. Preparation of PVDMA−Fe_3O_4 Nanoparticles. APTES−Fe_3O_4 (0.1 g) nanoparticles and 0.1 g of PVDMA were mixed in 20 mL of DCM, and the mixture was reacted at 25 °C for 24 h (Supporting Information Scheme S2). Then the product was washed several times by DCM and ethanol in sequence and dried under vacuum.

2.4.6. Preparation of L-Asparaginase−Fe_3O_4 Nanoparticles. PVDMA−Fe_3O_4 nanoparticles (10.0 mg) were mixed into 1 mL of L-asparaginase solution (3.5 mg/mL, 50.0 mM phosphate buffer, pH 8.6), and the mixture was agitated at 4 °C for required time (1−8 h, Supporting Information Scheme S2). After the immobilization reaction, the magnetic nanoparticles were retained by the magnet and stirred in 1.0 M ethanolamine in phosphate buffer (50.0 mM, pH 8.6) for 1 h to quench all unreacted azlactone functionalities.[11] Finally, the resultant magnetic nanoparticles were rinsed with the phosphate buffer (50.0 mM, pH 8.6) repeatedly to avoid the free enzyme, and the obtained L-asparaginase−Fe_3O_4 nanoparticles were stored in 50.0 mM Tris-HCl buffer (pH 8.6) at 4 °C for future usage.

2.5. Measurement of the Immobilized Amount of Enzyme. The amount of immobilized L-asparaginase was determined by a classical coomassie blue-binding assay. Coomassie brilliant blue G-250 (10.0 mg) was dissolved in 5 mL of 95% ethanol, and then 10 mL of 85% (w/v) phosphoric acid was added. The resulting solution was diluted by water to a final volume of 100 mL and filtered. After the immobilization reaction was stopped, the enzyme-modified magnetic nanoparticles were retained by a magnet. Then 20 μL of the supernatant solution was mixed with 180 μL of coomassie brilliant blue G-250 solution and the mixture was incubated for 2 min at 25 °C under shaking. The absorbance value at 595 nm was measured to calculate the immobilized amount of L-asparaginase on the magnetic nanoparticles using a SpectraMax M5 ELISA Reader (Molecular Devices, CA, USA). A calibration curve was obtained by monitoring the absorbance at 595 nm by the incubation reaction of a series of standard enzyme solutions with coomassie brilliant blue G-250 solution to allow accurate calculation of the immobilized amount.

2.6. Enzymolysis. The activity of the immobilized L-asparaginase was monitored by the developed CLE-CE protocol. As the specific substrate of L-asparaginase, asparagine (Asn) was dissolved in 50.0 mM Tri-HCl buffer (pH 8.6) and further diluted to desired concentrations. 0.4 mg of L-asparaginase-immobilized magnetic nanoparticles were mixed with 40 μL of enzyme substrate Asn solution in a 0.5 mL polypropylene tube and reacted at 37 °C for 1 min. Then the enzyme immobilized magnetic nanoparticles were retained by a magnet, and 20 μL of the supernatant solution was collected and further derived for CE analysis.

3. RESULTS AND DISCUSSION

3.1. Synthesis of the Reactive PVDMA. The azlactone ring of the VDMA is susceptible to the attack from nucleophiles and could efficiently produce stable covalent bonds under mild conditions.[9] Thus, PVDMA modified magnetic nanoparticles were considered to be potential templates for enzyme immobilization. In this study, a series of PVDMA brushes were synthesized through a RAFT polymerization process for 12−36 h using AIBN as initiator, CTAm as chain transfer agent and acetonitrile as solvent.[18,19] The monomer conversions and polymerization degree upon each different polymerization time were determined by NMR and the obtained results were presented in Table 1. Moreover, the molecular weight and polymer distribution index (PDI) of the resulting PVDMA were evaluated and the data was presented in Table 1. Although the molecular weight obtained from MOLDI-TOF MS and NMR was comparable, that obtained by GPC was lower. It should be mentioned that the same phenomenon has been reported in the literature.[23,24] It has been found that the molecular weight of PVDMA increased with the extension of

Scheme 1. Schematic Illustration of L-Asparaginase Immobilization onto PVDMA-Modified Magnetic Nanoparticles

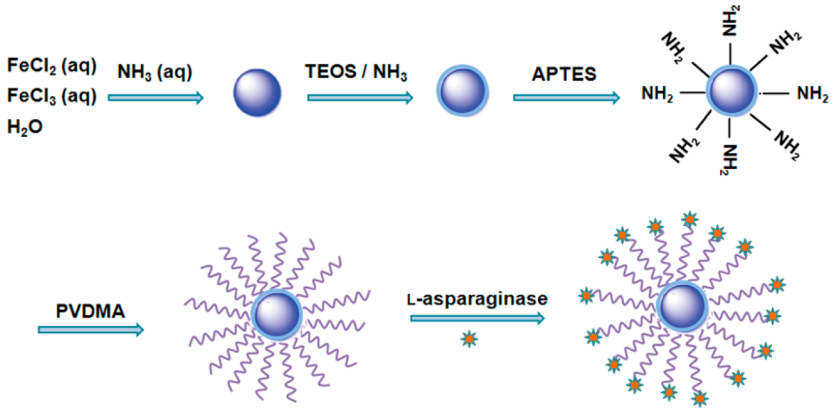

the polymerization time (Table 1), and further resulting in more reactive sites. The obtained PVDMA was thus applied to functionalize the magnetic nanoparticles for enzyme immobilization.

3.2. Preparation and Characterization of PVDMA–Fe_3O_4 Nanoparticles. The functional magnetic nanoparticles were prepared as presented in Scheme 1. First, the Fe_3O_4 nanoparticles were synthesized by the coprecipitation of Fe^{2+} and Fe^{3+} ions in ammonia solution as described by Massart and Cabuil.[21] Second, the Fe_3O_4 nanoparticles were coated with a silica shell to improve the modifiability and diminish the potential toxicity of bare magnetic nanoparticles[25−27] because the silica shell could protect Fe_3O_4 spheres from agglomeration and oxidation.[28] Next, the SiO_2–Fe_3O_4 nanoparticles were functionalized with APTES to produce the amino group. Then the reactive polymer PVDMA was grafted onto the amino-functionalized magnetic nanoparticles to endow them with the functionality for conjugating the enzyme.

Figure 1 showed the FT-IR spectra of Fe_3O_4, SiO_2–Fe_3O_4, PVDMA–Fe_3O_4 nanoparticles. The characteristic absorption of

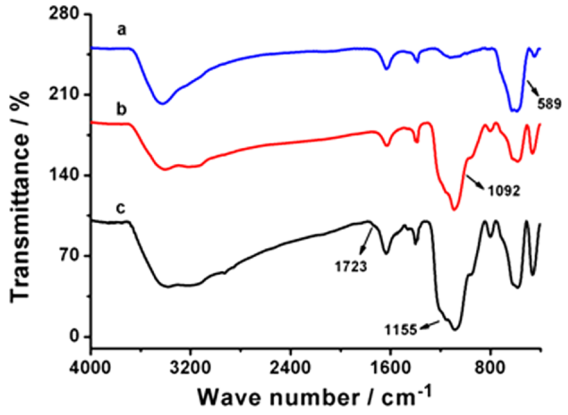

Figure 1. FT-IR spectra of Fe_3O_4 (a), SiO_2–Fe_3O_4 (b), and PVDMA–Fe_3O_4 (c) magnetic nanoparticles.

Fe–O from magnetic nanoparticles cores was observed at 589 cm^{-1}. The existence of the SiO_2 layer was validated by the typical peak of 1085 cm^{-1}, which was ascribed to the Si–O–Si antisymmetric stretching vibration. The PVDMA–Fe_3O_4 nanoparticles exhibited a characteristic signal of azlactone rings of VDMA units at 1803 cm^{-1} (C=O stretching) and 1195 cm^{-1} (C–O–C stretching), indicating that the reactive polymer PVDMA was successfully conjugated to the surface of the magnetic nanoparticles.[29,30]

Next, the morphology of the synthesized magnetic nanoparticles was characterized by TEM. As shown in Figure 2, the average diameter of Fe_3O_4 nanoparticles was 12.4 ± 0.3 nm, which was similar to the previous reports.[31,32] The grafting of the polymer did not obviously influence the size of the nanoparticles, and it was speculated that the PVDMA shell could not be distinguished in TEM images for the low contrast between polymer and the background,[31,33] In addition, a negative staining of the TEM sample was conducted to visualize the polymer coating by using PTA as staining agent, and the sample was observed by normal TEM. Only a thin layer around the magnetic nanoparticles could be observed (Supporting Information Figure S1). It was speculated that the polymer layer on the surface of the nanoparticles was limited and the negative staining agent PTA might be not effective for PVDMA polymer. However, the FT-IR results and the efficient immobilization of enzyme indeed identified the successful modification of PVDMA on the surface of the magnetic nanoparticles. Meanwhile, the DLS analysis was conducted to investigate the dispersity of the magnetic nanoparticles, and the results were presented in Supporting Information Table S1. It was obvious that the PDI of the magnetic nanoparticles was decreased from 0.785 to 0.302, indicating that the dispersity of the functionalized nanoparticles was improved.

The fraction of PVDMA polymer grafted onto the magnetic nanoparticles was determined by thermogravimetric analysis (TGA) method. The TGA curve was shown in Supporting Information Figure S2. It could be observed that there was a slight weight loss below 300 °C, which was probably caused by the loss of residual water.[34,35] Obvious weight loss for PVDMA–Fe_3O_4 nanoparticles was noticed between 300 and 560 °C, which was attributed to the degradation of PVDMA polymers on the surface of the magnetic nanoparticles. The results demonstrated that the amounts of PVDMA on the surface of the nanoparticles were estimated to be 2.4% (PVDMA-1–Fe_3O_4), 3.5% (PVDMA-2–Fe_3O_4) and 5.4% (PVDMA-3–Fe_3O_4), respectively.

The magnetic properties of the obtained magnetic nanoparticles at room temperature were investigated using a vibrating sample magnetometer (VSM). As displayed in Supporting Information Figure S3, the maximum saturation magnetization values of Fe_3O_4 nanoparticles, PVDMA–Fe_3O_4 nanoparticles, L-asparaginase–Fe_3O_4 nanoparticles were 73.1, 53.6, and 46.4 emu/g nanoparticles, respectively. Although the

dx.doi.org/10.1021/am5063025 | ACS Appl. Mater. Interfaces 2014, 6, 21346−21354

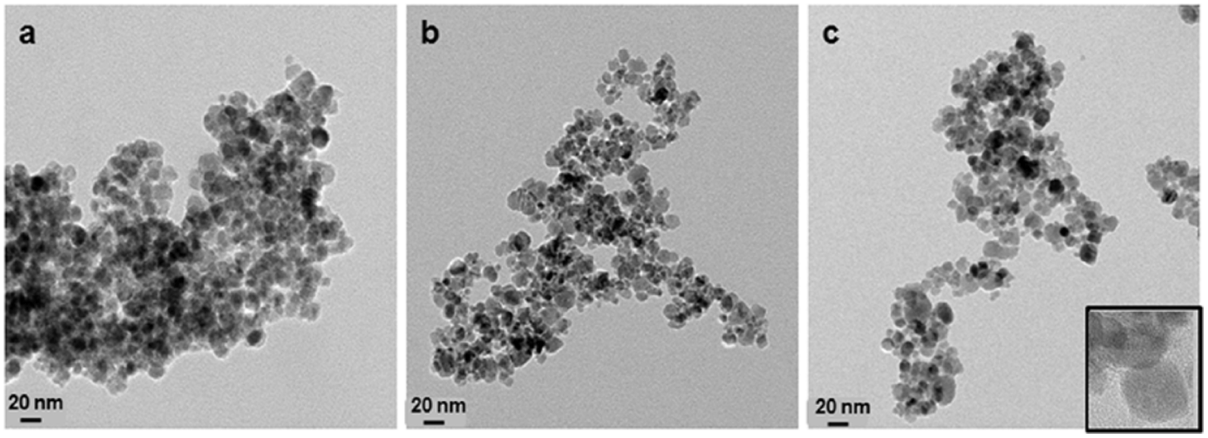

Figure 2. TEM images of (a) Fe_3O_4, (b) SiO_2−Fe_3O_4, and (c) PVDMA−Fe_3O_4 magnetic nanoparticles. (Inset: High-resolution TEM image of PVDMA−Fe_3O_4 magnetic nanoparticles.)

Table 2. Effect of the Grafted Chain Length on the Immobilized Amount of L-Asparaginase and the Activities of the Immobilized Enzyme

sample	immobilized amount of enzyme (μg mg^{-1} nanoparticle)	V_{max} (mM min^{-1})	K_m (mM)
free enzyme		0.11	0.70
L-asparaginase−Fe_3O_4-1[a]	107	1.45	0.56
L-asparaginase−Fe_3O_4-2[b]	276	1.47	0.61
L-asparaginase−Fe_3O_4-3[c]	318	1.54	0.67

[a]L-asparaginase−Fe_3O_4-1: the L-asparaginase reactor immobilized on PVDMA-1−Fe_3O_4 nanoparticles [b]L-asparaginase−Fe_3O_4-2: the L-asparaginase reactor immobilized on PVDMA-2−Fe_3O_4 nanoparticles [c]L-asparaginase−Fe_3O_4-3: the L-asparaginase reactor immobilized on PVDMA-3−Fe_3O_4 nanoparticles

magnetization of the nanoparticles decreased after modification, the magnetic response of these nanoparticles was still sufficient for further practical application. Additionally, we observed that the L-asparaginase−Fe_3O_4 nanoparticles could be rapidly separated from the solution with the assistance of an external magnet. Moreover, all these prepared nanoparticles possessed typical superparamagnetic behaviors with no obvious hysteresis and very low coercivity.[28,36]

3.3. Enzyme Immobilization. Since the azlactone functionalities could react readily with amine groups of the enzyme to form stable covalent bonds, the reactive polymer PVDMA-modified magnetic nanoparticles showed great potential to be favorable template for enzyme immobilization. L-Asparaginase has been extensively employed in the treatment of acute lymphoblastic leukemia; however, it might lead to some side effects (such as fever, allergic reactions, or anaphylactic shocks) and only circulate for limited time in the blood system. Therefore, the immobilization of native L-asparaginase was highly beneficial to reduce the immunological response, improve drug effect and prolong reaction time. In this study, the antileukemic enzyme L-asparaginase was chosen as the model enzyme and covalently conjugated on the PVDMA−Fe_3O_4 nanoparticles to construct an efficient enzyme reactor.

The classical coomassie blue-binding assay was employed to investigate the immobilization amount of L-asparaginase on the polymer-grafted magnetic nanoparticles as described in previous report.[32] First, the L-asparaginase solutions with various concentrations ranging from 0.015 to 5.0 mg/mL were incubated with Coomassie brilliant blue G-250 solution, and a calibration curve (Supporting Information Figure S4) was obtained by monitoring the absorbance at 595 nm. Then, the supernatant solutions before or after the immobilization were incubated with Coomassie brilliant blue G-250 solution and the immobilized amounts of enzyme were calculated according to the obtained calibration curve. Interestingly, as the data exhibited in Table 2, it has been found that the immobilized amount of enzyme increased (from 107 to 318 μg/mg nanoparticle) with the lengthened polymer chains, since more reaction sites were provided by these reactive polymer brushes. It was reported that the large surface/volume ratio of the polymer-grafted nanoparticles was favorable for higher loading capacity.[31,32] In this investigation, the immobilization efficiency (the calculation formula was displayed in Supporting Information) of the PVDMA-3−Fe_3O_4 nanoparticles reached 90.8%, thus it was chosen for further application. Compared with the previous reports, the synthesized PVDMA-modified magnetic nanoparticles were testified to be potential platform for enzyme immobilization in high loading capacity.[37−39]

Furthermore, the reaction time of the enzyme immobilization was optimized with PVDMA-3−Fe_3O_4 nanoparticles as a typical example, and the result was presented in Supporting Information Figure S5. The immobilized amount of enzyme was augmented with the reaction time increasing and then remained almost changeless after 4 h. Thus, 4 h was finally adopted as the optimum reaction time for enzyme immobilization.

3.4. Enzymolysis. Considering the interference from large amounts of L-AAs in complicated biological fluid, the study of L-asparaginase activity based on the determination of reactants made the chiral separation a key issue in the development of such methodology. After the successful construction of the enzyme reactor, a CLE-CE method was developed to study the kinetics of the immobilized enzyme due to its obvious advantages of high efficiency, low cost and convenient manipulation. In this proposed CLE-CE system, novel AAILs were synthesized and subsequently employed as efficient chiral

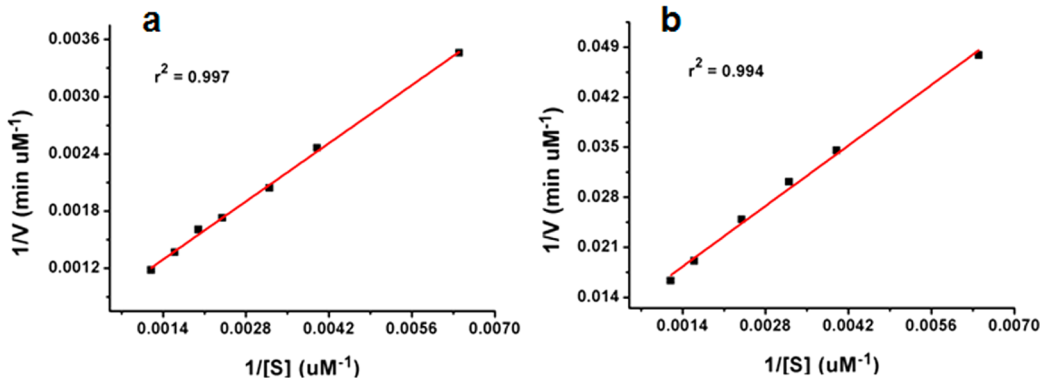

Figure 3. Lineweaver–Burk plot for (a) L-asparaginase immobilized magnetic nanoparticles modified with reactive polymer PVDMA and (b) free enzyme solution.

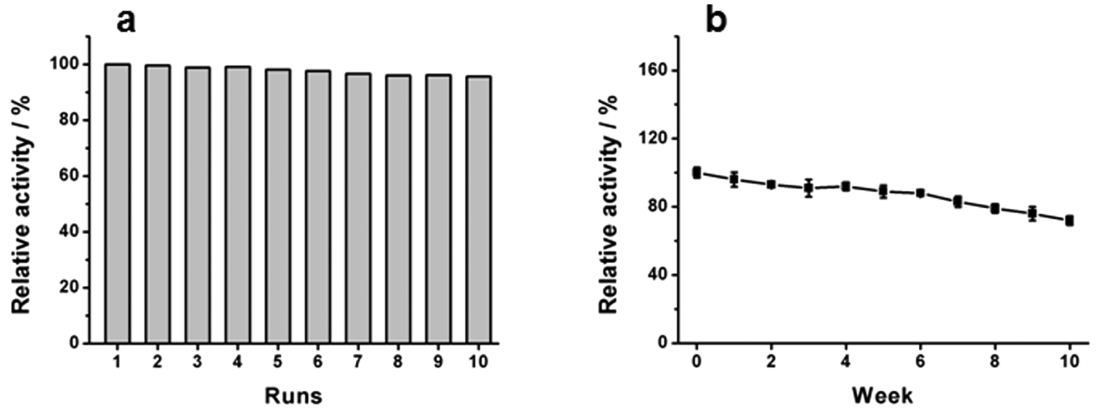

Figure 4. (a) Reusability test of L-asparaginase immobilized magnetic nanoparticles modified with reactive polymer and (b) stability test of L-asparaginase immobilized magnetic nanoparticles modified with reactive polymer.

ligands coordinated with Zn(II). The detail synthesis procedure and characterization results were provided in Supporting Information (Scheme S3). The effects of key parameters, including different kinds of AAILs, pH, concentration ratio of Zn(II) to chiral ligand and complex concentration, were investigated in detail, and the results were displayed in Supporting Information (Figure S6–S9). Under the optimum separation condition, 9 pairs of D,L-AAs including the substrate of L-asparaginase, D,L-Asn, were baseline-separated (Supporting Information Figure S10 and Table S2). The quantitative features of the proposed CLE-CE system were studied, and good linearity and favorable repeatability were obtained as the data was presented in Supporting Information. It should be noted that although the peak area of Dns-L-Asn decreased sharply after enzymatic reaction, the peak area of Dns-D-Asn maintained a constant level. This result strongly indicated that the present assay procedure could be used as a suitable platform for monitoring about L-asparaginase-mediated catalytic reaction.

The accurate measurement of rate constants which are associated with specific enzymatic reactions is quite significant for the application in biochemistry, medicine and food science.[40] L-Asn was the specific substrate of L-asparaginase, thus the values of Michaelis constant (K_m) and maximum velocity (V_{max}) were determined to investigate the enzymatic bioactivity of the enzyme reactor with L-Asn as the specific substrate using the proposed novel CLE-CE method. These values were obtained by ploting the initial reaction rate to the various substrate concentrations according to the linearized form of Michaelis–Menten equation as described following:[41]

$$[S]/v = K_m/V_{max} + [S]/V_{max}$$

where $[S]$ and v are the concentration of substrate and the velocity of the enzymatic reaction, respectively. K_m is the Michaelis constant which reflects the enzymatic affinities, and V_{max} is the maximum velocity which represents the activity of the enzyme reactor.

Figure 3a shows the plots for the conversion of L-Asn in the enzymatic reactions of the L-asparaginase–Fe_3O_4-3 reactor, and the corresponding kinetic characteristics are presented in Table 2. The K_m and V_{max} were calculated to be 0.67 mM and 1.54 mM min^{-1}, respectively. For comparison, the kinetic characteristics of free enzyme in solution were studied (Figure 3b), and the K_m and V_{max} values were 0.70 mM and 0.11 mM min^{-1}, respectively. It could be observed that the K_m value of the L-asparaginase immobilized on the PVDMA-modified magnetic nanoparticles was lower than that of native enzyme, indicating that the affinity between enzyme and its substrate was considerably enhanced when L-asparaginase was immobilized on magnetic nanoparticles.[12] Moreover, the V_{max} of the polymer-modified magnetic nanoparticles-based enzyme reactor was obviously higher than that of free enzyme, which means that a higher reaction rate for immobilized enzyme could be obtained at a similar concentration of substrate L-Asn in the solution.[41] This phenomenon was often observed for the immobilized enzyme systems and could be explained as follows: the plenty amount of L-asparaginase concentrated in limited space, and the diffusion within the matrix was decreased, further

Scheme 2. Simulation of Extracorporeal Shunt System Using the Enzyme Reactor Based on PVDMA-Modified Magnetic Nanoparticles

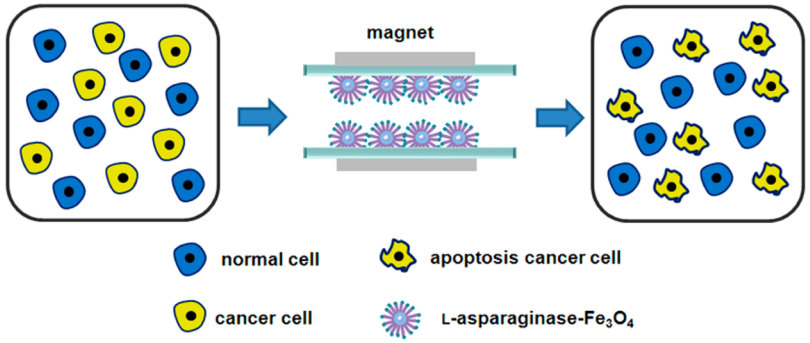

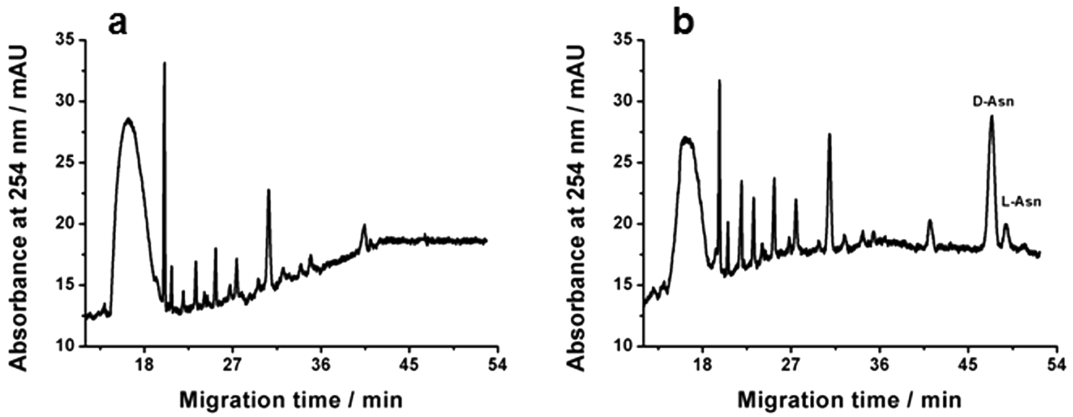

Figure 5. Electropherograms of hydrolyzation of L-Asn in human serum samples using L-asparaginase−Fe_3O_4 enzyme reactor as the simulation of an extracorporeal shunt system: (a) human serum sample and (b) human serum sample spiked with 500.0 μM D,L-Asn.

increasing the interaction frequency between the enzyme and the substrates.[42,43]

Furthermore, the influence of the polymer chains on the bioactivity of different enzyme reactors was investigated by studying the kinetic performance of them. As displayed in Table 2, the data demonstrated that the V_{max} increased from 1.45 to 1.54 mM min^{-1} with the increase of the polymer chain length, while the K_m value only slightly changed. Thus, we could infer that different polymer chain lengths might not exhibit obvious influence on the enzyme activity. However, in some extent, the increased polymer chains might be favorable for the enzymatic reaction because of the increased amount of immobilized enzyme.

3.5. Reusability and Stability. One of the most outstanding advantages of the enzyme reactors based on magnetic nanoparticles was that it could be used repeatedly. Thus, to estimate the reusability of the immobilized L-asparaginase based on polymer-modified magnetic nanoparticles, the substrate L-Asn was repeatedly incubated with the same group of the L-asparaginase−Fe_3O_4-3 nanoparticles. As the results shown in Figure 4a, we found that the immobilized enzyme could maintain more than 95.7% activity after being repeatedly operated for 10 times (time scale for 10 min). This result further validated its excellent biocompatibility of the PVDMA and its great capability for enzyme immobilization. Moreover, the stability of the immobilized enzyme was investigated by storing it in the Tris-HCl buffer (50.0 mM, pH 8.6), and the results were displayed in Figure 4b. This enzyme reactor based on PVDMA-modified magnetic nanoparticles kept more than 72.6% activity after 10 weeks storage. However, the native L-asparaginase only retained 20.3% activity after 4 weeks at the same storage condition. These results demonstrated that the storage stability of L-asparaginase was greatly improved after being immobilized onto the PVDMA-modified magnetic nanoparticles. This phenomenon could be explained as follows: after the enzyme was immobilized to a carrier, its freedom to undergo drastic conformational changes was limited, resulting in the increased stability against denaturation.[44] Since the proposed L-asparaginase reactor possessed favorable biocompatibility, good stability and outstanding reusability, it was considered to have great potential for application in an extracorporeal shunt system for acute lymphoblastic leukemia treatment.

3.6. Simulation of Extracorporeal Shunt System. Since L-asparaginase is testified to be an effective antitumor agent, especially for acute lymphoblastic leukemia. Recently, the extracorporeal shunt system with immobilized enzyme reactor has received increasing attention for it paves entirely new way for leukemia treatment and is proved to be very prospective in the future leukemia treatment. Thus, it was significant to explore biocompatible materials for L-asparaginase immobilization. It has been reported that magnetic nanoparticles with smaller size did not accumulate in the reticuloendothelial system (RES).[45] Moreover, the biocompatible coating like PEG could enable the magnetic nanoparticles to escape the RES system.[46] Since PVDMA or L-asparaginase was biocompatible molecules and the size of the magnetic nanoparticles were less than 15 nm, therefore, it was speculated that the functionalized magnetic nanoparticels could evade the RES system when they were introduced into the biological systems. In this study,

human serum samples were incubated with the L-asparaginase reactor based on polymer-grafted magnetic nanoparticles to evaluate its potential in clinical application as shown in Scheme 2. Since the concentration of L-Asn in serum was approximately from 30.0 to 60.0 μM,[47−49] the substrate L-Asn was completely depleted during the enzymolysis process as displayed in Figure 5a. Thus, 833.0 μM D,L-Asn was spiked in the serum sample and further incubated with the enzyme reactor. As illustrated in Figure 5b, it could be observed that the concentration of the substrate L-Asn decreased significantly because of the enzymolysis of the fabricated enzyme reactor. To further promote the clinical application, the L-asparaginase reactor based on polymer-grafted magnetic nanoparticles was incubated with acute lymphoblastic leukemia cells (JurkatE6-1), and the apoptosis of cells was analyzed by fluorescence activated cell sorter (FACS). Compared with control, the incubation of the cells with L-asparaginase reactor was sufficient to drive apoptosis as the results shown in Supporting Information Figure S11. All of the results demonstrated that the proposed L-asparaginase reactor based on PVDMA−Fe_3O_4 nanoparticles could be developed as the potential material applied in clinical treatment of acute lymphoblastic leukemia.

4. CONCLUSION

In this work, we have successfully synthesized PVDMA by RAFT polymerization and the PVDMA-modified magnetic nanoparticles were developed as an effective template for L-asparaginase immobilization. The affinity of the immobilized L-asparaginase increased considerably compared with that of free enzyme. Furthermore, because of the increased amount of the immobilized enzyme, the longer the polymer chains were, the more favorable for the enzymatic reaction was. The prepared enzyme reactor presented favorable reusability and long-term stability. Meanwhile, an extracorporeal shunt system was simulated, showing its potential application in leukemia treatment. This report illustrated that the reactive polymer-modified magnetic nanoparticles were promising platform for enzyme immobilization in high efficiency, and the present techniques paved a new platform for the design of efficient enzyme reactors applicable in clinical treatments.

■ ASSOCIATED CONTENT

Supporting Information

The RAFT synthesis process of PVDMA, the enzyme immobilization process, the synthesis process of AAILs, NMR characterization of AAILs, the TEM image of PVDMA-3−Fe_3O_4 magnetic nanoparticles by using PTA as staining agent, the DLS analysis results, thermogravimetric analysis of magnetic nanoparticles, magnetization curves of magnetic nanoparticles, the calibration curve of L-asparaginase by the classical coomassie blue-binding assay, the effect of the reaction time on the enzyme immobilization process, separation condition optimization, the electropherogram of Dns-D,L-Phe, Dns-D,L-Ser, Dns-D,L-Asn, enantioseparation results of Dns-D,L-AAs under the optimum CLE-CE conditions, apoptosis analysis using FACS after Annexin V-FITC/PI staining of JurkatE6−1 cells, and the quantitative analysis results of D,L-Asn. This material is available free of charge via the Internet at http://pubs.acs.org.

■ AUTHOR INFORMATION

Corresponding Author

*Tel: +86-10-82627290. Fax: +86-10-62559373. E-mail: qili@iccas.ac.cn.

Notes

The authors declare no competing financial interest.

■ ACKNOWLEDGMENTS

This work is supported by grants from the NSFC (Nos. 21375132, 21175138, 21135006, and 21321003) and National Basic Research Program of China (No. 2015CB932001). Also, we greatly appreciate Dr. Jian Hou and Prof. Zongxiu Nie for their kind help in the MS analysis. Moreover, we appreciate Dr. Nan Zhang, Linlin Wang, Dr. Suyan Liu, Dr. Mingxia Jiao, Yuming Zhao, Prof. Dihua Shangguan, Prof. Fuyi Wang, Prof. Mingyuan Gao, and Prof. Ke Zhang for their kind help.

■ REFERENCES

(1) Zhou, Z.; Hartmann, M. Progress in Enzyme Immobilization in Ordered Mesoporous Materials and Related Applications. *Chem. Soc. Rev.* **2013**, *42*, 3894−3912.
(2) Chao, C.; Liu, J. D.; Wang, J. T.; Zhang, Y. W.; Zhang, B.; Zhang, Y. T.; Xiang, X.; Chen, R. F. Surface Modification of Halloysite Nanotubes with Dopamine for Enzyme Immobilization. *ACS Appl. Mater. Interfaces* **2013**, *5*, 10559−10564.
(3) Ma, J. F.; Zhang, L. H.; Liang, Z.; Zhang, W. B.; Zhang, Y. K. Recent Advances in Immobilized Enzymatic Reactors and Their Applications in Proteome Analysis. *Anal. Chim. Acta* **2009**, *632*, 1−8.
(4) Kim, J.; Grate, J. W.; Wang, P. Nanostructures for Enzyme Stabilization. *Chem. Eng. Sci.* **2006**, *61*, 1017−1026.
(5) Qin, W. J.; Song, Z. F.; Fan, C.; Zhang, W. J.; Cai, Y.; Zhang, Y. J.; Qian, X. H. Trypsin Immobilization on Hairy Polymer Chains Hybrid Magnetic Nanoparticles for Ultra Fast, Highly Efficient Proteome Digestion, Facile ^{18}O-Labeling and Absolute Protein Quantification. *Anal. Chem.* **2012**, *84*, 3138−3144.
(6) Huang, S. H.; Juang, R. S. Biochemical and Biomedical Applications of Multifunctional Magnetic Nanoparticles: A Review. *J. Nanopart. Res.* **2011**, *13*, 4411−4430.
(7) Konwarh, R.; Karak, N.; Rai, S. K.; Mukherjee, A. K. Polymer-Assisted Iron Oxide Magnetic Nanoparticle Immobilized Keratinase. *Nanotechnology* **2009**, *20*, 225107.
(8) Heilmann, S. M.; Rasmussen, J. K.; Krepski, L. R. Chemistry and Technology of 2-Alkenyl Azlactones. *J. Polym. Sci., Part A: Polym. Chem.* **2001**, *39*, 3655−3677.
(9) Cullen, S. P.; Mandel, I. C.; Gopalan, P. Surface-Anchored Poly(2-Vinyl-4,4-dimethyl azlactone) Brushes as Templates for Enzyme Immobilization. *Langmuir* **2008**, *24*, 13701−13709.
(10) Peterson, D. S.; Rohr, T.; Svec, F.; Fréchet, J. M. J. Enzymatic Microreactor-on-a-Chip: Protein Mapping Using Trypsin Immobilized on Porous Polymer Monoliths Molded in Channels of Microfluidic Devices. *Anal. Chem.* **2002**, *74*, 4081−4088.
(11) Krenkova, J.; Lacher, N. A.; Svec, F. Highly Efficient Enzyme Reactors Containing Trypsin and Endoproteinase LysC Immobilized on Porous Polymer Monolith Coupled to MS Suitable for Analysis of Antibodies. *Anal. Chem.* **2009**, *81*, 2004−2012.
(12) Zhang, Y. Q.; Tao, M. L.; Shen, W. D.; Zhou, Y. Z.; Ding, Y.; Ma, Y.; Zhou, W. L. Immobilization of L-Asparaginase on the Microparticles of the Natural Silk Sericin Protein and Its Characters. *Biomaterials* **2004**, *25*, 3751−3759.
(13) Agrawal, N. R.; Bukowski, R. M.; Rybicki, L. A.; Kurtzberg, J.; Cohen, L. J.; Hussein, M. A. A Phase I−II Trial of Polyethylene Glycol-Conjugated L-Asparaginase in Patients with Multiple Myeloma. *Cancer* **2003**, *98*, 94−99.
(14) Allison, J. P.; Davidson, L.; Gutierrez-Hartman, A.; Kitto, G. B. Insolubilization of L-Asparaginase by Covalent Attachment to Nylon Tubing. *Biochem. Biophys. Res. Commun.* **1972**, *47*, 66−73.

(15) Hrvath, C.; Sardi, A.; Woods, J. S. L-Asparaginase Tubes: Kinetic Behavior and Application in Physiological Studies. *J. Appl. Physiol.* **1973**, *34*, 181−187.
(16) Bernath, F. R.; Olanoff, L. S.; Vieth, W. R. Therapeutic Perspectives of Enzyme Reactors. In *Biomedical Applications of Immobilized Enzymes and Proteins*, Vol. *1*; Chang, T. M. S., Ed.; Plenum Press: New York, 1977; pp 351−375.
(17) Mu, X. Y.; Qi, L.; Qiao, J.; Yang, X. Z.; Ma, H. M. Enantioseparation of Dansyl Amino Acids and Dipeptides by Chiral Ligand Exchange Capillary Electrophoresis Based on Zn(II)-L-Hydroxyproline Complexes Coordinating With γ-Cyclodextrins. *Anal. Chim. Acta* **2014**, DOI: 10.1016/j.aca.2014.07.022.
(18) Lai, J. T.; Filla, D.; Shea, R. Functional Polymers from Novel Carboxyl-Terminated Trithiocarbonates as Highly Efficient RAFT Agents. *Macromolecules* **2002**, *35*, 6754−6756.
(19) Zhu, Y. C.; Quek, J. Y.; Lowe, A. B.; Roth, P. J. Thermoresponsive (Co)Polymers through Postpolymerization Modification of Poly(2-Vinyl-4,4-dimethylazlactone). *Macromolecules* **2013**, *46*, 6475−6484.
(20) Quek, J. Y.; Zhu, Y. C.; Roth, P. J.; Davis, T. P.; Lowe, A. B. RAFT Synthesis and Aqueous Solution Behavior of Novel pH- and Thermo-Responsive (Co)Polymers Derived from Reactive Poly(2-Vinyl-4,4-dimethylazlactone) Scaffolds. *Macromolecules* **2013**, *46*, 7290−7302.
(21) Massart, R.; Cabuil, V. Effect of Some Parameters on the Formation of Colloidal Magnetite in Alkaline Medium: Yield and Particle Size Control. *J. Chim. Phys. Phys.-Chim. Biol.* **1987**, *84*, 967−973.
(22) Jiang, Y. Y.; Guo, C.; Xia, H. S.; Mahmood, I.; Liu, C. Z.; Liu, H. Z. Magnetic Nanoparticles Supported Ionic Liquids for Lipase Immobilization: Enzyme Activity in Catalyzing Esterification. *J. Mol. Catal. B: Enzym.* **2009**, *58*, 103−109.
(23) Ferreira, M. L.; Galland, G. B.; Damiani, D. E.; Villar, M. A. FTIR, ^{13}C NMR, and GPC Analysis of High-Propylene Content Co- and Terpolymers with Ethylene and Higher α-Olefins Synthesized with $EtInd_2ZrCl_2$/MAO. *J. Polym. Sci., Part A: Polym. Chem.* **2001**, *39*, 2005−2018.
(24) Hou, S. S.; Kuo, P. L. Synthesis and Characterization of Amphiphilic Graft Copolymers Based on Poly(Styrene-co-maleic Anhydride) with Oligo(Oxyethylene) Side Chains and Their GPC Behavior. *Polymer* **2001**, *42*, 2387−2394.
(25) Corr, S. A.; Rakovich, Y. P.; Gun'ko, Y. K. Multifunctional Magnetic-Fluorescent Nanocomposites for Biomedical Applications. *Nanoscale Res. Lett.* **2008**, *3*, 87−104.
(26) Donselaar, L. N.; Philipse, A. P. Interactions between Silica Colloids with Magnetite Cores: Diffusion, Sedimentation and Light Scattering. *J. Colloid Interface Sci.* **1999**, *212*, 14−23.
(27) Shen, Y.; Zhao, L. Z.; Qi, L.; Qiao, J.; Mao, L. Q.; Chen, Y. Reactive Polymer as a Versatile Toolbox for Construction of Multifunctional Superparamagnetic Nanocomposites. *Chem.—Eur. J.* **2012**, *18*, 13755−13761.
(28) Liu, Q.; Shi, J. B.; Cheng, M. T.; Li, G. L.; Cao, D.; Jiang, G. B. Preparation of Graphene-Encapsulated Magnetic Microspheres for Protein/Peptide Enrichment and MALDI-TOF MS Analysis. *Chem. Commun.* **2012**, *48*, 1874−1876.
(29) Pray-in, Y.; Rutnakornpituk, B.; Wichai, U.; Vilaivan, T.; Rutnakornpituk, M. Hydrophilic Azlactone-Functionalized Magnetite Nanoparticle for Conjugation with Folic Acid. *J. Nanopart. Res.* **2014**, *16*, 2357.
(30) Prai-in, Y.; Tankanya, K.; Rutnakornpituk, B.; Wichai, U.; Montembault, V.; Pascual, S.; Fontaine, L.; Rutnakornpituk, M. Azlactone Functionalization of Magnetic Nanoparticles using ATRP and Their Bioconjugation. *Polymer* **2012**, *53*, 113−120.
(31) Shen, Y.; Guo, W.; Qi, L.; Qiao, J.; Wang, F. Y.; Mao, L. Q. Immobilization of Trypsinviareactive Polymer Grafting from Magnetic Nanoparticles for Microwave-Assisted Digestion. *J. Mater. Chem. B* **2013**, *1*, 2260−2267.
(32) Mu, X. Y.; Qiao, J.; Qi, L.; Liu, Y.; Ma, H. M. Construction of D-Amino Acid Oxidase Reactor Based on Magnetic Nanoparticles Modified by a Reactive Polymer and Its Application in Screening Enzyme Inhibitors. *ACS Appl. Mater. Interfaces* **2014**, *6*, 12979−12987.
(33) Luo, B.; Song, X. J.; Zhang, F.; Xia, A.; Yang, W. L.; Hu, J. H.; Wang, C. C. Multi-Functional Thermosensitive Composite Microspheres with High Magnetic Susceptibility Based on Magnetite Colloidal Nanoparticle Clusters. *Langmuir* **2010**, *26*, 1674−1679.
(34) Hussein-Al-Ali, S. H.; Zowalaty, M. E. E.; Hussein, M. Z.; Ismail, M.; Dorniani, D.; Webster, T. J. Novel Kojic Acid-Polymer-Based Magnetic Nanocomposites for Medical Applications. *Int. J. Nanomed.* **2014**, *9*, 351−362.
(35) Chen, J. P.; Yang, P. C.; Ma, Y. H.; Tu, S. J.; Lu, Y. J. Targeted Delivery of Tissue Plasminogen Activator by Binding to Silica-Coated Magnetic Nanoparticle. *Int. J. Nanomed.* **2012**, *7*, 5137−5149.
(36) Wan, S. R.; Zheng, Y.; Liu, Y. Q.; Yan, H. S.; Liu, K. L. Fe_3O_4 Nanoparticles Coated with Homopolymers of Glycerol Mono(Meth)-Acrylate and Their Block Copolymers. *J. Mater. Chem.* **2005**, *15*, 3424−3430.
(37) Bava, A.; Gornati, R.; Cappellini, F.; Caldinelli, L.; Pollegioni, L.; Bernardini, G. D-Amino Acid Oxidase-Nanoparticle System: A Potential Novel Approach for Cancer Enzymatic Therapy. *Nanomedicine* **2013**, *8*, 1797−1806.
(38) Lin, S.; Yun, D.; Qi, D. W.; Deng, C. H.; Li, Y.; Zhang, X. M. Novel Microwave-Assisted Digestion by Trypsin-Immobilized Magnetic Nanoparticles for Proteomic Analysis. *J. Proteome Res.* **2008**, *7*, 1297−1307.
(39) Krogh, T. N.; Berg, T.; Højrup, P. Protein Analysis Using Enzymes Immobilized to Paramagnetic Beads. *Anal. Biochem.* **1999**, *274*, 153−162.
(40) Ristenpart, W. D.; Wan, J.; Stone, H. A. Enzymatic Reactions in Microfluidic Devices: Michaelis-Menten Kinetics. *Anal. Chem.* **2008**, *80*, 3270−3276.
(41) Wu, H. L.; Tian, Y. P.; Liu, B. H.; Lu, H. J.; Wang, X. Y.; Zhai, J. J.; Jin, H.; Yang, P. Y.; Xu, Y. M.; Wang, H. H. Titania and Alumina Sol-Gel-Derived Microfluidics Enzymatic-Reactors for Peptide Mapping: Design, Characterization, and Performance. *J. Proteome Res.* **2004**, *3*, 1201−1209.
(42) Bi, H. Y.; Qiao, L.; Busnel, J. M.; Liu, B. H.; Girault, H. H. Kinetics of Proteolytic Reactions in Nanoporous Materials. *J. Proteome Res.* **2009**, *8*, 4685−4692.
(43) Jiang, D. S.; Long, S. Y.; Huang, J.; Xiao, H. Y.; Zhou, J. Y. Immobilization of *Pycnoporus* Sanguineuslaccase on Magnetic Chitosan Microspheres. *Biochem. Eng. J.* **2005**, *25*, 15−23.
(44) Leonowicz, A.; Sarkar, J. M.; Bollag, J. M. Improvement in Stability of an Immobilized Fungal Laccase. *Appl. Microbiol. Biotechnol.* **1988**, *29*, 129−135.
(45) Khandhar, A. P.; Ferguson, R. M.; Arami, H.; Krishnan, K. M. Monodisperse Magnetite Nanoparticle Tracers for in Vivo Magnetic Particle Imaging. *Biomaterials* **2013**, *34*, 3837−3845.
(46) Qiao, R. R.; Yang, C. H.; Gao, M. Y. Superparamagnetic Iron Oxide Nanoparticles: From Preparations to in Vivo MRI Applications. *J. Mater. Chem.* **2009**, *19*, 6274−6293.
(47) Taylor, C. W.; Dorr, R. T.; Fanta, P.; Hersh, E. M.; Salmon, S. E. A Phase I and Pharmacodynamic Evaluation of Polyethylene Glycol-Conjugated L-Asparaginase in Patients with Advanced Solid Tumors. *Cancer Chemother. Pharmacol.* **2001**, *47*, 83−88.
(48) Jackson, J. A.; Halvorson, H. R.; Furlong, J. W.; Lucast, K. D.; Shore, J. D. A New Extracorporeal Reactor-Dialyzer for Enzyme Therapy Using Immobilized L-Asparaginase. *J. Pharmacol. Exp. Ther.* **1979**, *209*, 271−274.
(49) Qiao, J.; Qi, L.; Mu, X. Y.; Chen, Y. Monolith and Coating Enzymatic Microreactors of L-Asparaginase: Kinetics Study by MCE−LIF for Potential Application in Acute Lymphoblastic Leukemia Treatment. *Analyst* **2011**, *136*, 2077−2083.